



ENHANCEMENT OF AEROACOUSTIC TESTING IN CLOSED-SECTION WIND TUNNELS

Yara M. Hinssen¹, Roberto Merino-Martínez¹, and Niels L. S. Moonen²

¹Faculty of Aerospace Engineering, Delft University of Technology
Kluyverweg 1, 2629 HS Delft, The Netherlands.

²Flow Technology Department, Peutz B.V.
Lindenlaan 41, 6584 AC Molenhoek, The Netherlands.

Abstract

Aeroacoustic testing in wind tunnels is crucial for understanding and mitigating the noise generation mechanisms in several devices while maintaining satisfactory aerodynamic performance during the design stage. However, current aeroacoustic measurements in closed-section wind tunnels face challenges in terms of installation of acoustic sensors, due to the effect of the boundary layer of the wind tunnel walls, and accuracy. To address these issues, the proposed methodology integrates advanced signal processing techniques and cost-effective and limited alterations in a closed-section wind tunnel. Different setup configurations combined with the use of a microphone array consisting of 88 microphones, recessed behind an acoustically transparent stainless steel mesh, have led to significant improvements in signal-to-noise ratio and measurement accuracy compared to the baseline single microphone aeroacoustic testing capabilities. These configurations included a perforated panel with incorporated windscreens, a perforated panel with melamine foam rings, and the addition of melamine foam panels behind the array and inside the wind tunnel, along one of its walls. In general, the proposed approach enables the identification of noise sources with a signal-to-noise ratio of at least -10 dB. Additionally, the utilisation of advanced beamforming techniques (CLEAN-SC and DAMAS) in post-processing yields clearer outcomes. Finally, the effectiveness of the setup was evaluated, using a realistic test model, resulting in an approximate 15 dB improvement in peak prominence, with respect to single-microphone measurements, of a tonal flow-induced noise source due to the higher number of microphones and the application of beamforming.

1 INTRODUCTION

In recent years, there has been a growing emphasis on sustainability in various societal and environmental aspects, such as aviation [1], industrial development, and mobility. As a result, in-

terest in mitigating noise pollution and nuisance has also increased over time [2]. With the transition towards more sustainable energy sources, such as wind energy and its accompanying wind turbines [3], the increase in air traffic, and the rise in urban development there are now more aeroacoustic noise sources that produce flow-induced noise than ever [4]. These sources can have a detrimental impact on the environment and public health. According to the World Health Organisation (WHO), noise pollution is one of the biggest health risks in city life¹. Aeroacoustics is the field of study concerned with flow-induced noise, and, therefore, aeroacoustic testing during the design stage is of utmost importance to minimise the noise annoyance of the resulting designs. Aeroacoustic tests can be performed in wind tunnels, which have been proven and validated for conducting experiments on smaller-scale models and in aerodynamically controlled environments. While computational analysis methods like computational aeroacoustics (CAA) may provide accurate results, they are still modelled and not experimentally validated. Additionally, a high level of geometrical detail is required for aeroacoustic testing, especially because small details can be responsible for high-frequency noise, which is computationally expensive. On the other hand, full-scale and/or field tests can be very costly and may not yet be available during earlier design stages. Therefore, wind tunnel testing, with scaled models if necessary, can be a practical compromise solution for aeroacoustic testing.

However, aeroacoustic testing in a wind tunnel is not straightforward, as most conventional wind tunnels are optimised for aerodynamic performance and the acoustic performance is typically not the main point of interest. As a result, wind tunnels are often noisy environments with many different noise sources coming from the flow, reflections, fans, etc. Therefore, research to improve aeroacoustic testing in a (closed-section) wind tunnel can lead to a better understanding of the aeroacoustic phenomena that occur during testing and can lead to better results to modify designs for lower noise production [5].

Many advancements have been made over the years leading to a broad base of available steps and improvements to ensure good aeroacoustic testing results [6–8]. The current research employs the closed-section atmospheric boundary layer wind tunnel at Peutz B.V. as a baseline facility to investigate potential improvements. Research was conducted on various types of hardware, such as different types of microphones, data acquisition systems, and structural components of the setup, including microphone arrays. To ensure a simple approach that can be easily implemented by researchers at wind tunnel facilities, a readily available commercial microphone array was used to perform the measurements. Furthermore, the measurement setup was based on previously found options to improve aeroacoustic testing in wind tunnels [9]. In these other research projects, multiple alterations were tested and led to promising results. These alterations included placing microphones recessed in cavities, behind an acoustically transparent metal mesh sheet as shown by VanDercreek [9], wall treatments [10–12], and using hybrid test sections [10, 13]. These alterations were further analysed and used to design the setup for the experimental campaign of this research.

Lastly, different post-processing methods were researched and analysed to provide the best possible system for data analysis. Here, conventional frequency domain beamforming (CF-DBF) was used as the baseline, and more advanced methods, such as CLEAN-SC [14, 15] and DAMAS [16], were considered to further improve the obtained acoustic results.

In conclusion, this paper aims to present the research that was conducted to find a cost-

¹<https://ec.europa.eu/research-and-innovation/en/horizon-magazine/noise-pollution-one-biggest%2Dhealth-risks-city-life>

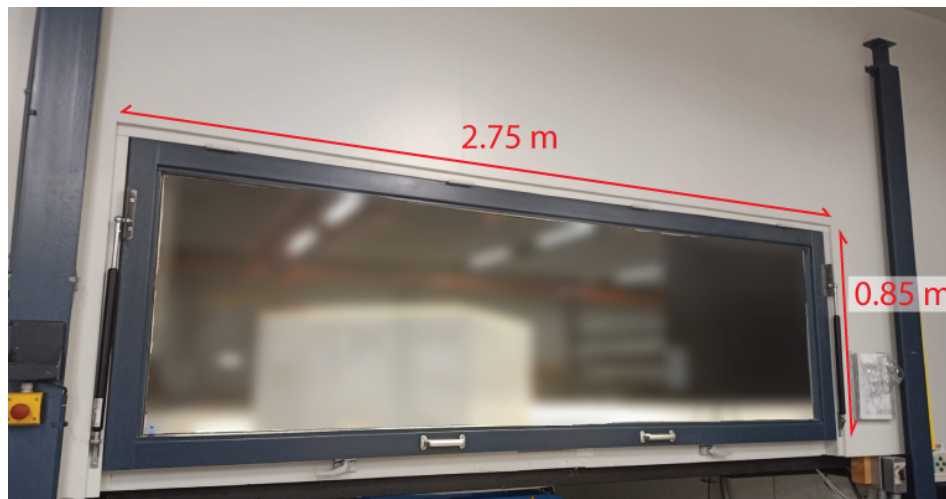


Figure 1: Peutz B.V. wind tunnel showing window location and its dimensions.

effective, easy, and flexible way to enhance the aeroacoustic testing capabilities of a conventional closed-section wind tunnel in which the main focus is on the microphone array placement while applying minimal alterations to the wind tunnel.

This manuscript is structured as follows: Section 2 describes the experimental setup employed, including the wind-tunnel facility and the setups and measurement equipment employed. The acoustic imaging methods considered in this paper are briefly explained in section 3. Section 4 discusses the main experimental results, including those regarding tests with a speaker and a fence. Lastly, the conclusions and recommendations are gathered in section 5. This manuscript is a summary of the main findings reported in the MSc thesis of Yara M. Hinssen. For further details, the reader is referred to the original full document [17].

2 EXPERIMENTAL SETUP

2.1 Wind-tunnel facility

The experimental study was conducted at the wind tunnel facility at Peutz B.V., in Mook, The Netherlands. This closed-section, closed-circuit wind-tunnel facility measures approximately $26.5 \text{ m} \times 10 \text{ m}$ (length \times width), with a test section of $3.2 \text{ m} \times 3.2 \text{ m} \times 1.80 \text{ m}$ (in length \times width \times height). It is powered by four axial fans providing a flow velocity at the test section up to a maximum of approximately 25 m/s . The test section has a transparent glass window that can be opened that is 2.75 m in length and 0.85 m in height, see Figure 1. This facility is mostly used for research regarding wind in the urban environment, wind pressures, dispersion of substances, and aero- and hydrodynamic research for offshore projects². The segment upstream from the test section can be altered using inserts which leads to different atmospheric boundary layer properties. For acoustic testing, these inserts are removed and an empty wind tunnel is used.

²<https://www.peutzgroup.com/index.php/node/56>

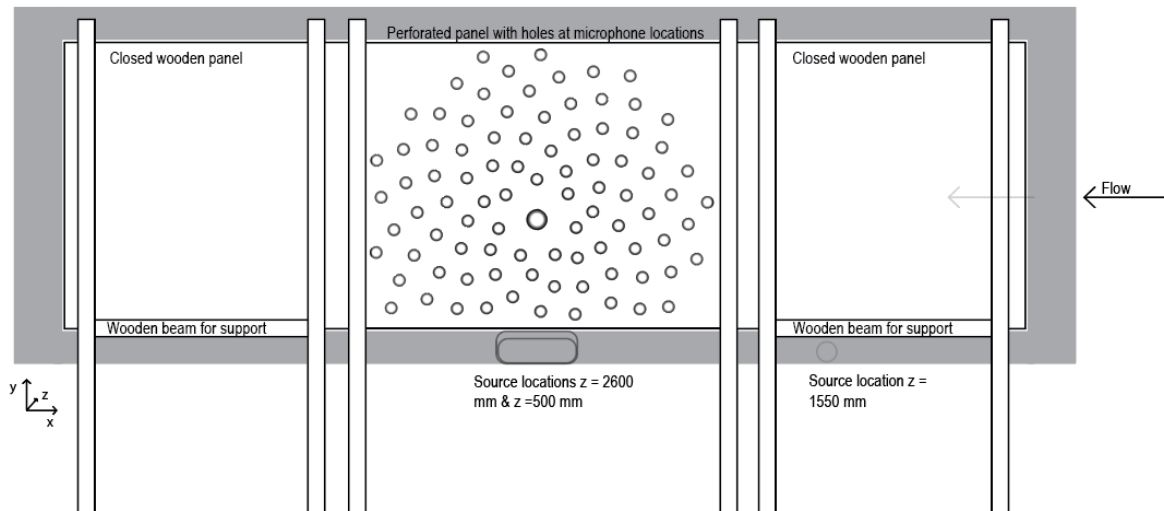


Figure 2: Structural setup used during tests, side view seen from outside the wind tunnel. Note: Setup 1 does not use the middle segment as displayed.

2.2 Measurement device

The tests were performed with the CAE Bionic M-112³ microphone array and the measurements were recorded using the CAE Noise Inspector software. This array consists of 112 MEMS microphones equipped with spherical windscreens and measures 1 m in diameter. Of these 112 microphones, only 88 had an unobstructed view of the test section throughout the setups employed in this study and were, henceforth, employed in the analysis. The microphone array has a 24-bit resolution, a sampling frequency of 48 kHz, and a nominal frequency range between 10 Hz and 24 kHz. For each measurement, a recording time of 10 s was employed.

2.3 Microphone array placements

A test setup was built consisting of three separate segments that cover the full window area of the wind tunnel. The main goal of this was to ensure that none of the parts would become structurally unstable or too heavy to handle by a single person. The two segments, or stands, on the outer sides, were purely designed to ensure a proper closed-section wind tunnel. They were constructed out of 2 MDF (medium-density fibreboard) wooden panels, one measuring 870 mm × 840 mm × 18 mm (length × height × thickness) and one measuring 880 mm × 840 mm × 18 mm (in length × height × thickness) respectively, held up by 2 wooden beams that were placed on the floor next to the tunnel. The length of the load-bearing poles was adjusted to ensure the segments were clamped in place to then be taped off on the inside to prevent any air gaps or holes. The middle segment was altered to test multiple setups. For this segment, three different setups were devised. The full setup, as seen from outside of the tunnel is displayed in Figure 2.

³<https://www.cae-systems.de/en/products/acoustic-camera-sound-source-localization/bionic-m-112.html>

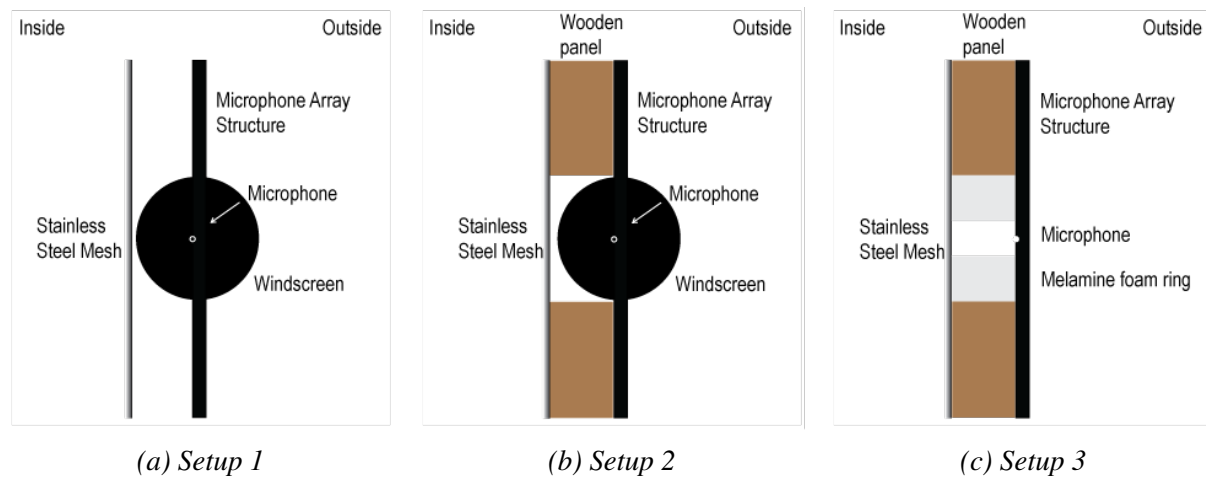


Figure 3: Visual representation of the cross-section of the three different setups employed.

In Figure 3 the cross-sections of the three test setups are displayed. In the first setup, it was attempted to create an aerodynamically-closed, yet acoustically-open test section (i.e. a hybrid test section) [10] by using a 500 thread per square inch (#500) stainless steel cloth with a thread diameter of 0.026 mm and placing the measurement device directly behind it with the windscreens placed just behind the mesh. This mesh was adhered to the side panels and top and bottom edges of the wind tunnel and kept in place for all three test setups. For the second test setup, an MDF panel with the same thickness as the side panels was clamped in between the side panels with circular holes of 36 mm diameter at the exact locations of the microphones in the measurement device. The windscreens of the CAE Bionic M-112 microphone array were pushed into the cut-outs to further close the test section and ensure the microphones were aligned with the cut-outs. The last test setup, setup three (3), used the same perforated panel as setup two (2), however, this time the original windscreens were removed from the microphone array. Instead, melamine rings with an outer diameter of 36 mm, an inner diameter of 9 mm, and a thickness of 20 mm were placed into the holes after which the microphone array was aligned and attached to the panel. These three setups were then tested using two experimental campaigns, described in sections 2.5 and 2.6.

2.4 Melamine foam additions

In addition to the three different setups previously described, the implementation of a melamine foam back panel, attached to the back of the microphone array, was tested to evaluate whether this would lead to further improvements by further attenuating the potential background noise outside of the wind tunnel. This panel was made to fit between the wooden beams and includes cut-outs for the hardware and measures approximately 1000 mm × 840 mm × 80 mm (width × height × thickness). Lastly, a test was performed with melamine foam panels with a total dimension of 2400 mm × 1400 mm × 50 mm (width × height × thickness) placed on the wind tunnel wall opposite the microphone array to assess whether this would decrease reflections without drastic alterations to the wind tunnel aerodynamic performance. Pictures of the setups and melamine foam additions on the back of the array can be found in Figure 4.

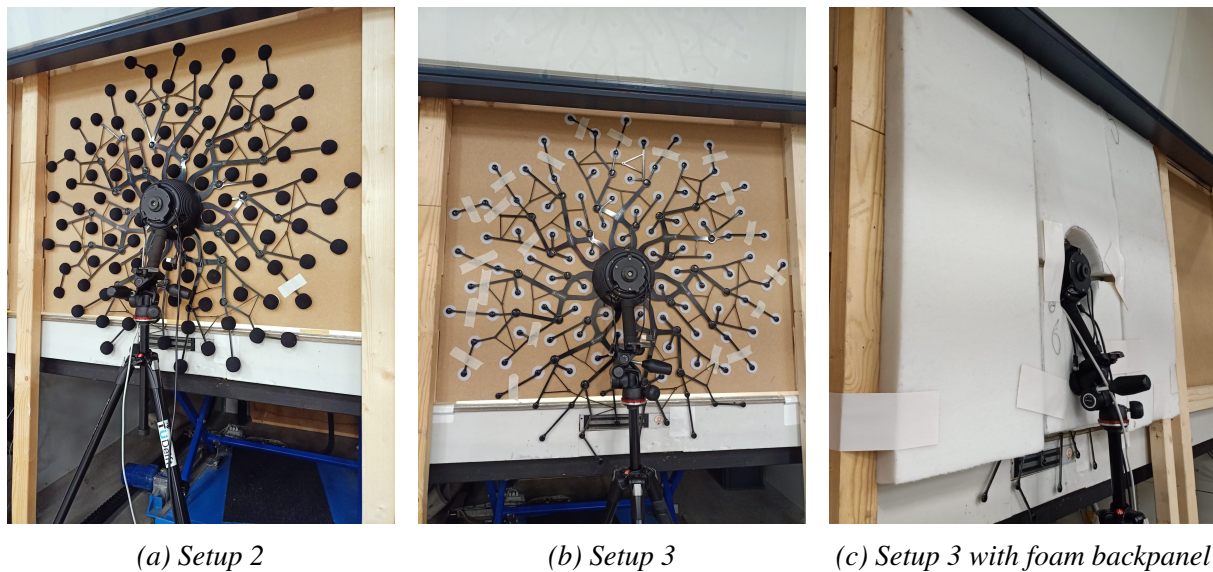


Figure 4: Pictures of the different setups.

2.5 Speaker Experiment

Measurements were performed with three different flow velocities (5 m/s, 10 m/s, and 15 m/s), using a JBL Charge 5 speaker emitting white noise. This speaker measures 220 mm × 96 mm × 93 mm (length × width × height), has a power of 40 W, and a nominal frequency range from 60 Hz to 20 kHz. The relatively small and streamlined shape of the speaker is expected to generate relatively low flow-generated noise compared to the white noise signal employed. It was placed on the turntable on the floor of the wind tunnel, enabling different source locations. For this study, only one speaker location at a distance of 2.6 m away from the array plane was considered. In addition, background measurements of the wind tunnel, and measurements without flow were performed to obtain the expected true signals. A visual representation of the test section and the different speaker locations can be seen in Figure 5a. The presented results all have use the source location furthest from the array as highlighted in Figure 5a.

2.6 Fence Experiment

Moreover, tests were performed to evaluate the applicability of the proposed test setup. To accomplish that, two previously-analysed test subjects (two different bridge fences), were placed in the wind tunnel and the different array setups were used (see Figure 5b). Here the main focus was on the comparison to the previously reported results by Peutz B.V. using a single microphone flush-mounted into the floor of the same wind tunnel. This microphone was a Bruël & Kjaer 2250 single-channel class 1 sound level meter⁴. The results were primarily compared by focusing on the recorded frequency spectra of the wind tunnel and the test subject. During this study, the fences were tested for several flow velocities and sideslip angles between the fences and the flow to replicate the conditions of the original tests.

⁴<https://www.bksv.com/en/instruments/handheld/sound-level-meters/2250-series>

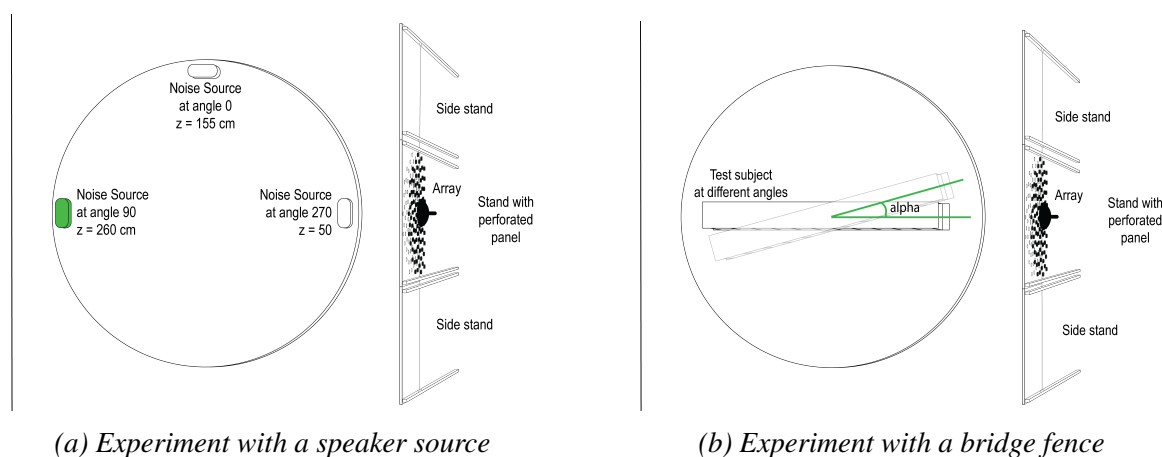


Figure 5: Visualisations of the two experimental campaigns in the wind tunnel seen from above.

3 METHODOLOGY

3.1 Conventional Beamforming (CFDBF)

Using the data acquired during the experimental campaigns, various methods of post-processing were applied to further improve the results. All the data was analysed using Welch's method [18] with time blocks of 4096 samples, Hanning windowing, and a 50% overlap. The scan grid used for the measurements spans the entire wind tunnel test section with a grid spacing of 50 mm. The speaker source results displayed in this paper all consider a distance from the array plane of 2.60 m. For the fence measurements, the chosen distance from the array plane was 1.55 m. Additionally, a 200 mm \times 200 mm square region of integration (ROI) was defined for all measurements depending centered on the sound source location for performing source power integration [19, 20].

Cross-Spectral Matrix (CSM) manipulation

In addition, diagonal removal (DR) of the cross-spectral matrix was used to decrease the effect of incoherent noise and, therefore, decrease the influence of background noise. This DR was used for all the results unless when explicitly stated. This method replaces all of the values in the main diagonal of the CSM with zeroes which eliminates much of the incoherent noise.

Furthermore, diagonal optimisation (DOpt) of the CSM was applied to assess its improvement compared to the original CSM without the potential nonphysical results that might be obtained by using DR [21]. For this, the method proposed by Hald [22] was used in which the diagonal is optimised to be as close to zero as possible while adhering to the positive-definite eigenvalues. This is performed by convex (CVX) optimisation in which a diagonal vector is added to the CSM. This is then minimised, which would lead to lower values of incoherent noise. Lastly, it was analysed whether subtracting the CSM of a background measurement without a sound source (i.e. the empty tunnel) from the CSM of a measurement with the same wind tunnel and setup properties including a sound source would improve the results. This subtraction is performed for every frequency on every band that is analysed.

3.2 Advanced deconvolution methods

CLEAN-SC [14], was also used to further analyse the results from the experimental campaigns with a loop gain of 0.99 and a clean beamwidth of 0.0125 cm. Lastly, DAMAS [16] (Deconvolution Approach for the Mapping of Acoustic Sources) was applied with a maximum amount of iterations of 250 and 500 to further analyse the effect of this advanced beamforming method on the results. Both methods were applied to cases without CSM manipulation and DR.

4 RESULTS AND DISCUSSION

4.1 Speaker Experiment

From the original tests, it was found that setup 1 already performs adequately from a localisation perspective. The localisation of the source worsens at higher frequencies where the wind tunnel background noise is much louder than the noise source leading to negative signal-to-noise ratio (SNR) values. In Figure 6a, the sound pressure level (SPL or L_p) is displayed for the white noise sound source, as well as the background at a flow velocity of 10 m/s. Here, it can be seen that at 2500 Hz (denoted with a vertical black dashed line), the SNR is approximately -10 dB. Using CFDBF, the source maps at a one-third-octave band (T.O.B.) centered at that frequency still clearly show the noise source, as can be seen in Figure 6b.

Setups 2 and 3 show similar source plots, as can be seen in Figure 6c and 6d. Using these setups the recorded L_p was decreased, however, also the measured sound signals from the sound source were attenuated. Especially for white noise cases, in which the SNR at higher frequencies was negative, this would explain the lack of improvement in the source plots. In general, a quantitative study of the SNR improvement provided by each test Setup showed little to no difference between the three Setups considered here. The enhancement with respect to a baseline with a single microphone or a flush-mounted microphone array is still relevant, but the differences between setups in terms of results were minor.

4.2 Fence Experiment

The applicability study, using the bridge fences, yielded additional results that provide evidence of the measurement setup and strategy's proof of concept. The commercial real-time beamforming software from the CAE array successfully detected and located a source of noise during the live analysis, as shown in Figure 7. This same location was found during the post-processing of the measurement, see Figure 8.

This noise localisation can not be performed with a single microphone and as such the proposed method broadens the aeroacoustic testing capabilities.

Furthermore, the prominence of the peak is increased which can be attributed to the improvement in SNR due to the increased number of microphones. In Figure 9 the T.O.B. spectra obtained using the current method and their integrated counterpart are visible, as well as the results from the original test reported by Peutz B.V. with a single microphone. Here, a peak prominence of approximately 30 dB is found for the 1600 Hz source compared to its neighbouring frequency bands. This is approximately 12-15 dB larger than found during the original tests as reported by Peutz B.V.

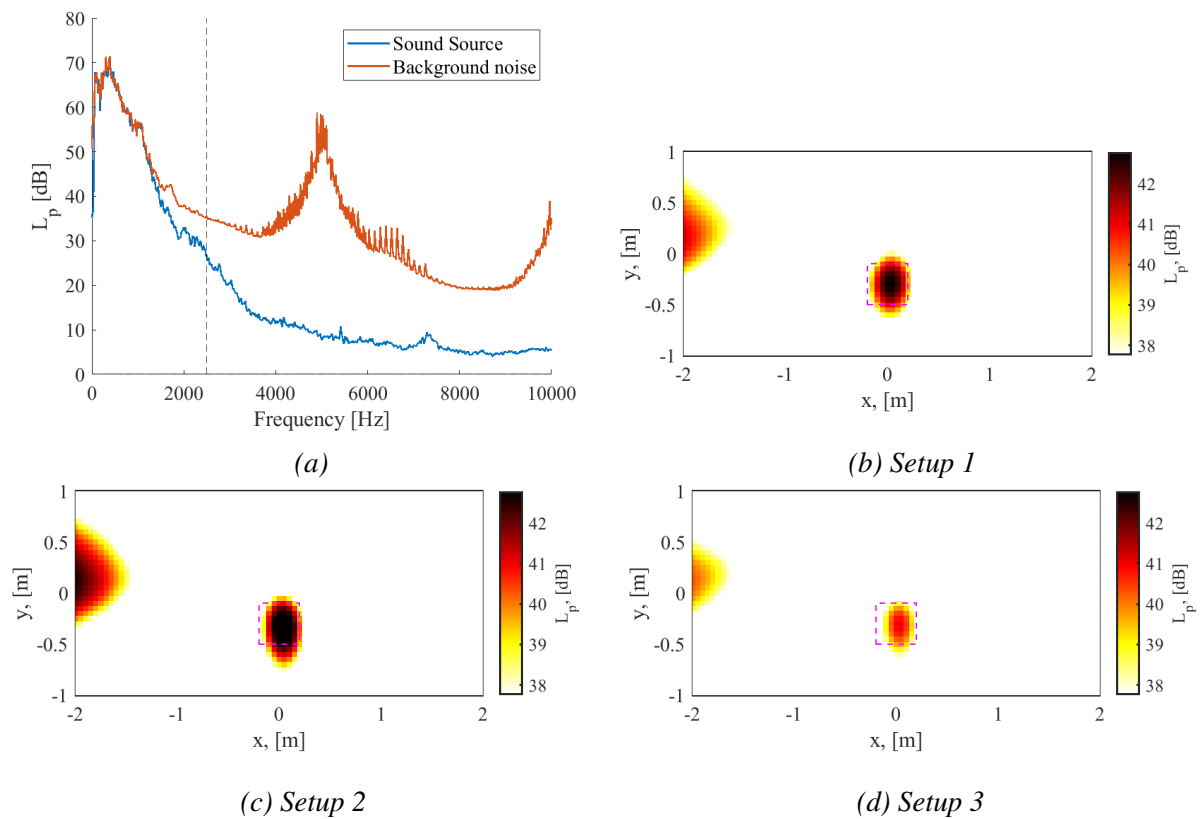


Figure 6: (a) Frequency spectra of the white noise source (speaker) and the background noise at $V = 10$ m/s when using Setup 1. (b-d) CFDBF acoustic source maps of the white noise source analysed on a T.O.B. centered at 2500 Hz using different setups and a flow velocity $V = 10$ m/s. The dashed magenta square denotes the ROI.

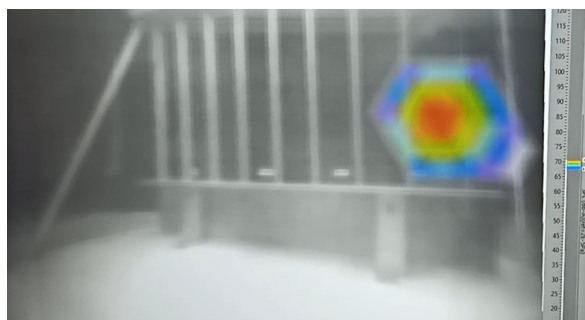


Figure 7: Real-time beamforming in CAE Noise Inspector Software at Z distance 1.5 m.

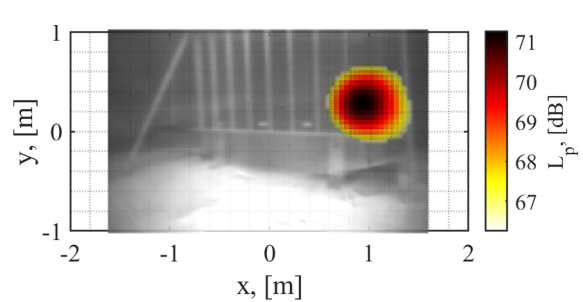


Figure 8: Source plot of the fence analysed on a T.O.B. centred at 1600 Hz, using CFDBF, flow velocity $V = 8$ m/s.

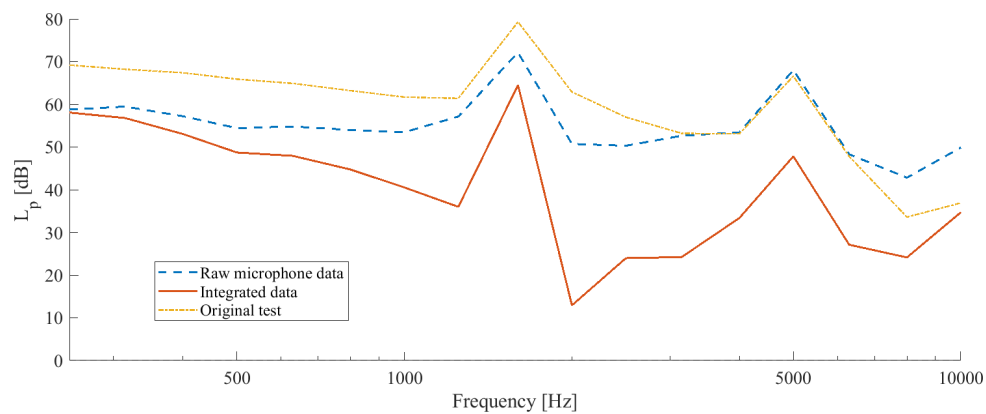


Figure 9: Integrated T.O.B. Spectra compared to results from original Peutz B.V. tests with one microphone.

4.3 Melamine foam additions

As explained before, two other additions using melamine foam were tested during the verification tests to evaluate whether they could further improve the results. The results of these two additions can be found below in Figure 10. These graphs show that the melamine foam has a positive impact in localising the noise source and identifying the reflections. It also shows that the melamine rings in setup 3 absorb more sound than the windscreens in setup 2 leading to a lower peak level of the speaker source.

Lastly, the addition of the melamine panel to the wall opposite the microphone array improves the localisation and reduces to some extent the reflection on the wind tunnel floor. Furthermore, a reason for the slight increase in peak level compared to setup 3 in Figure 10c, and Figure 10d, could be that the absorption of the sound reflections prevents destructive interference at this particular frequency.

4.4 Advanced deconvolution methods

Applying different advanced deconvolution methods to the measurement results led to clearer results and can assist in clarifying the location of the noise sources. To understand the influence of the background noise, Figure 11 shows the same source at different velocities. The source in these graphs is a speaker emitting white noise.

As can be seen in Figure 11d, at a flow velocity of 15 m/s, using CFDBF and DR, it is possible to identify the noise source but there is background noise contamination in the graph.

These results can be improved by using the advanced deconvolution methods CLEAN-SC and DAMAS.

In Figure 12 it can be seen that both methods clean up the results and eliminate most of the background noise. However, given the longer computational time and the coarser grid size required by the DAMAS method, CLEAN-SC appears to be the most efficient method. Furthermore, DAMAS shows a dominant sound source with a higher peak level at the top left of the grid, which is not shown by CLEAN-SC.

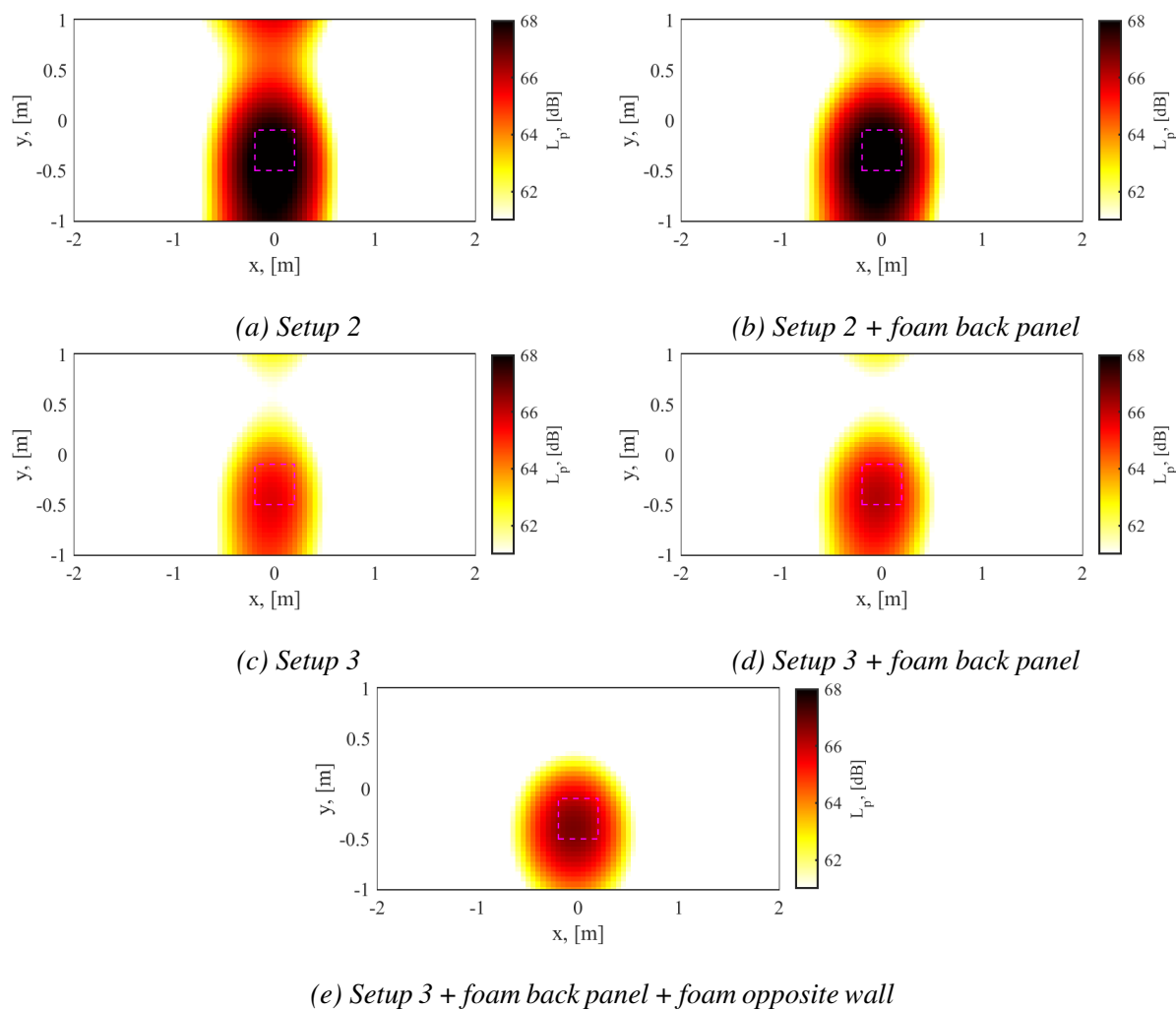


Figure 10: CFDBF acoustic source maps analysed on a T.O.B. centred at 1000 Hz at a flow velocity $V = 5$ m/s using the different setups. The dashed magenta square denotes the ROI.

CSM manipulation

As can be seen from Figure 13b, this effect is very limited for this specific case and frequency. Furthermore, a case was analysed in which the CSM of a background measurement without a sound source was subtracted from the CSM of measurement with the sound source. This improves the results significantly as can be seen in Figure 13d.

Lastly, the advanced deconvolution methods were applied to a case in which no CSM manipulation was performed to assess their effect. In Figure 14, it can be seen that CLEAN-SC manages to locate the source but has a secondary source in the top left. DAMAS locates a primary source at this top left location but cannot locate the speaker source without the application of CSM manipulation.

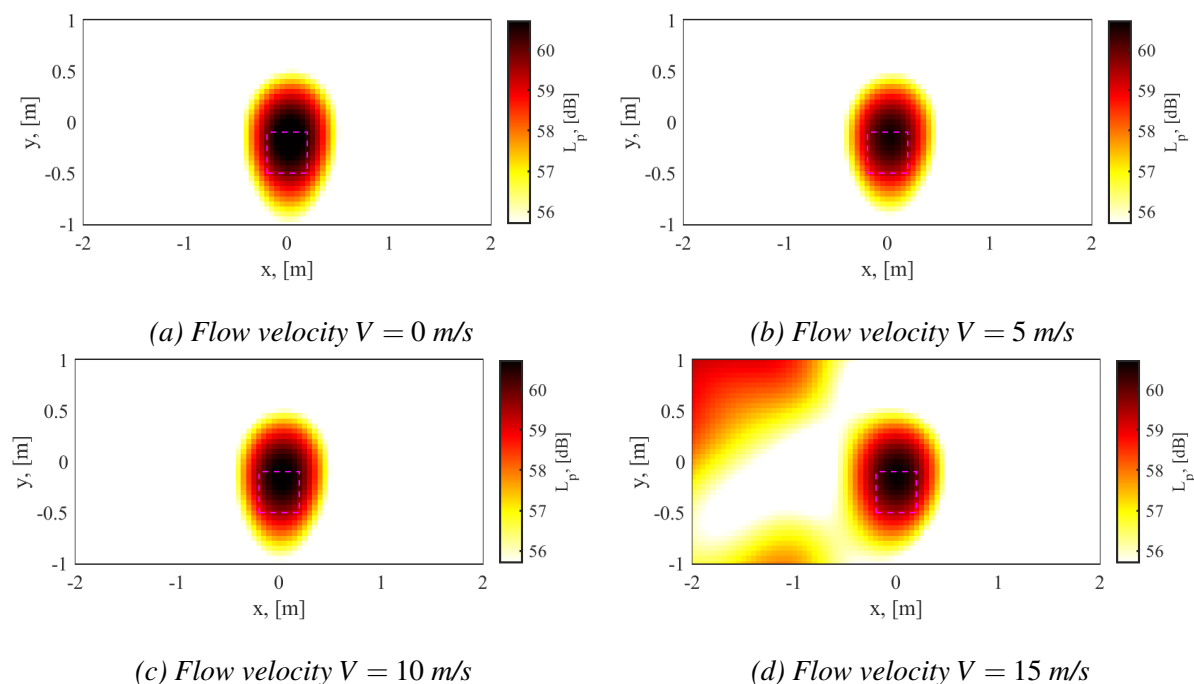


Figure 11: CFDBF acoustic source maps of the white noise sound source analysed on a T.O.B. centred at 1250 Hz using Setup 1, DR, and different flow velocities. The dashed magenta square denotes the ROI.

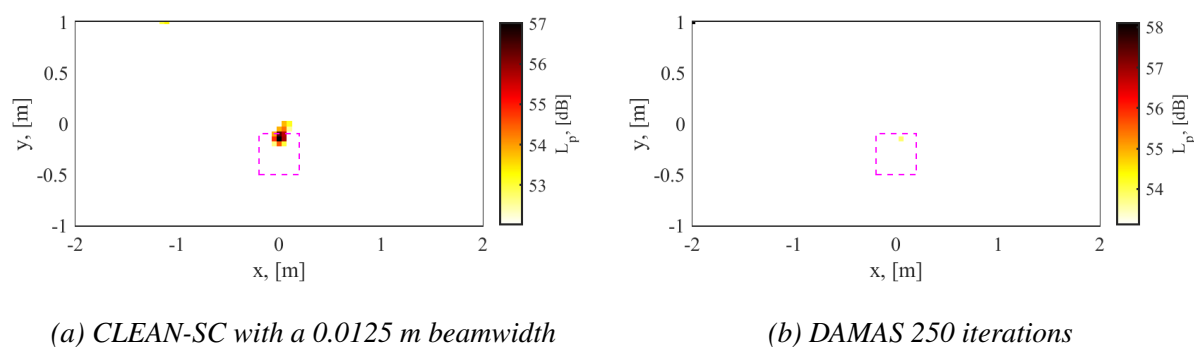


Figure 12: Acoustic source maps of white noise sound source analysed on a T.O.B. centred at 1250 Hz, flow velocity $V = 15$ m/s, using Setup 1, DR, and different deconvolution methods. The dashed magenta square denotes the ROI.

5 CONCLUSIONS AND RECOMMENDATIONS

To allow for the mitigation of noise pollution, aeroacoustic testing in the early design stage of products or structures could be a helpful tool. However, given the challenging application of aeroacoustic testing in closed-section wind tunnels, and the difficulties as a result of aerodynamic (and not acoustic) optimisation of wind tunnel facilities, a relatively simple and cost-effective way of aeroacoustic testing is necessary. Therefore, this research aimed to investigate to what extent simple setups combined with a microphone array and different data analysis

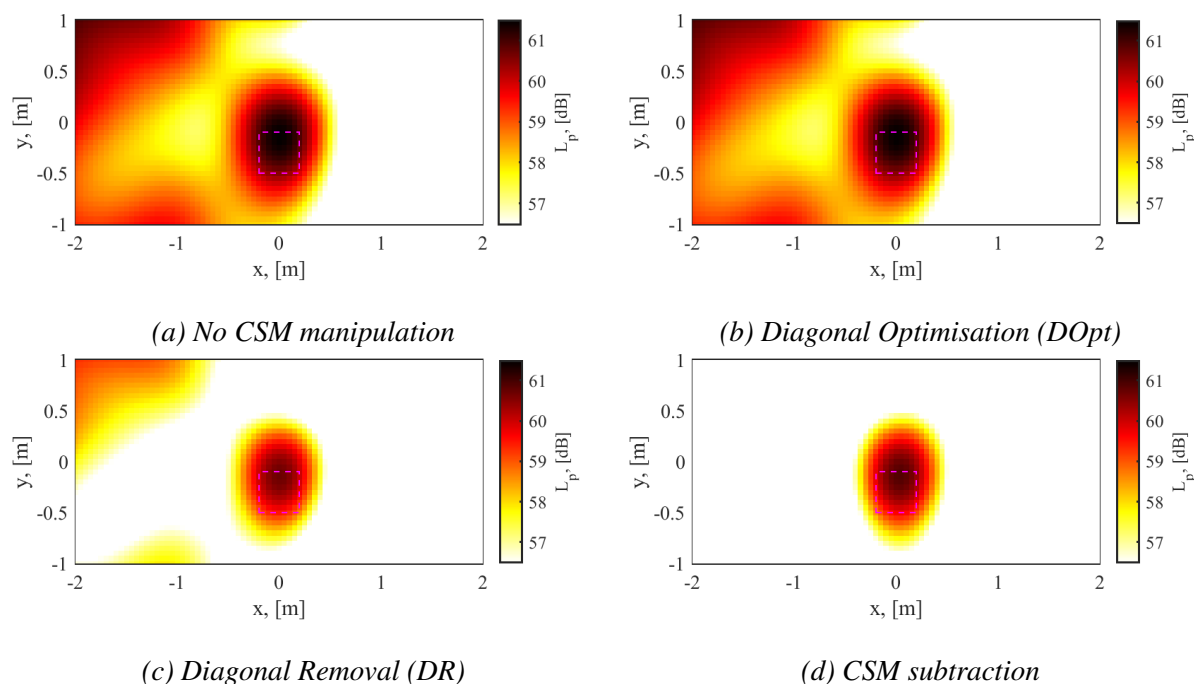


Figure 13: CFDBF acoustic source maps of white noise sound source analysed on a T.O.B. centred at 1250 Hz, flow velocity $V = 15$ m/s, using Setup 1 and different CSM diagonal manipulation methods. The dashed magenta square denotes the ROI.

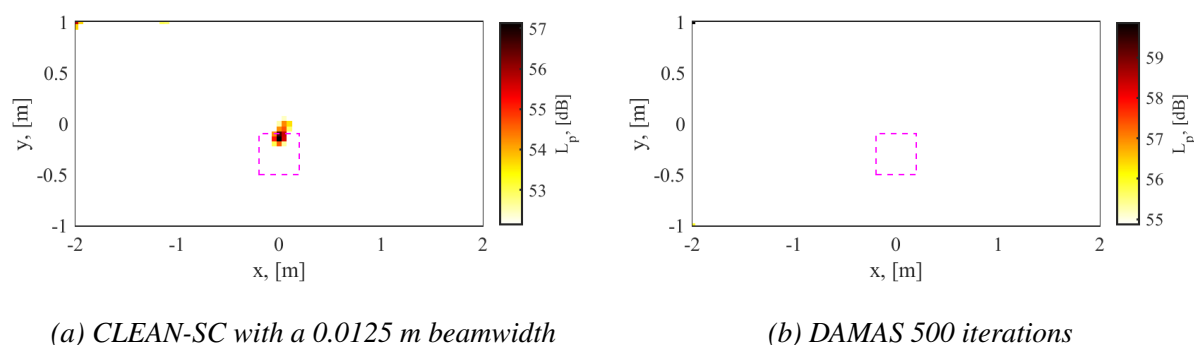


Figure 14: Acoustic source maps of white noise sound source analysed on a T.O.B centred at 1250 Hz, flow velocity $V=15$ m/s, using Setup 1, no diagonal manipulation and different deconvolution methods. The dashed magenta square denotes the ROI.

methods could provide this improvement in aeroacoustic testing. From the results discussed before, it can be concluded that with relatively simple and cost-effective alterations to a closed-section wind tunnel, aeroacoustic testing with a microphone array can be performed involving sound source localisation provided that the SNR is at least -10 dB. These results can then be further improved using deconvolution methods to increase precision which is partly dictated by chosen parameters. Simple alterations to the wind tunnel setup can help to reduce the background noise, but for the sound signals tested, the decrease in the measured sound source was nearly the same leading to almost no improvement in signal-to-noise ratio. It would however be

interesting to test more, especially higher-frequency, sound sources to evaluate whether, in that case, the SNR might be increased by the setups. Additionally, this research has proved valuable in the analysis of an application case with a realistic test subject (a fence) where this method of aeroacoustic testing correctly identified the frequencies of flow-induced noise and increased their peak prominence by up to 15 dB.

Using a different sound source, with a higher SNR, as well as more tonal noise measurements at higher frequencies, specifically with lower SNRs could complement the results and provide a more complete overview of the true applicability of the used method. Additionally, given the location of the noise source on the wind tunnel floor, the results were prone to many reflections, which might be reduced by placing the noise source at a different location in the wind tunnel, which is also more realistic for typical test subjects. Lastly, a quiet surrounding outside of the wind tunnel is of utmost importance to prevent corrupted measurements for which further improvements to the setup by enclosing the array on the outside could provide better and cleaner results.

ACKNOWLEDGEMENTS

This research project has been realized with a financial contribution of the province of Limburg (“provincie Limburg”). Additionally, this publication is also a part of the *Listen to the future* project (project number 20247), a part of the Veni 2022 research programme (Domain Applied and Engineering Sciences) granted to Roberto Merino-Martinez and is also (partially) financed by NWO.

provincie limburg



Ministerie van Economische Zaken
en Klimaat

References

- [1] R. Merino-Martinez, J. Kennedy, and G. J. Bennett. ‘Experimental study of realistic low-noise technologies applied to a full-scale nose landing gear.’ *Aerospace Science and Technology*, 113(106705), 1–20, 2021. doi:10.1016/j.ast.2021.106705. URL <https://www.sciencedirect.com/science/article/pii/S1270963821002157?via%3Dihub>.
- [2] Y. Zhou, V. Valeau, J. Marchal, F. Ollivier, and R. Marchiano. ‘Three-dimensional identification of flow-induced noise sources with a tunnel-shaped array of mems microphones.’ *Journal of Sound and Vibration*, 482, 115459, 2020. ISSN 0022-460X. doi: <https://doi.org/10.1016/j.jsv.2020.115459>.

- [3] R. Merino-Martinez, R. Pieren, and B. Schäffer. ‘Holistic approach to wind turbine noise: From blade trailing–edge modifications to annoyance estimation.’ *Renewable and Sustainable Energy Reviews*, 148(111285), 1–14, 2021. doi:10.1016/j.rser.2021.111285. URL <https://doi.org/10.1016/j.rser.2021.111285>.
- [4] J. Ploemen, L. Nijs, A. Pleysier, and R. Schipper. ‘Wind-induced sound on buildings and structures.’ 2011. ISBN 9781907132339. 13th International Conference on Wind Engineering.
- [5] S. Janssen, H. Vos, A. Eisses, and E. Pedersen. ‘Predicting annoyance by wind turbine noise.’ 2010. Internoise, 39th International congress of noise control engineering; Conference date: 13-06-2010 Through 16-06-2010.
- [6] A. Cigada, M. Lurati, F. Ripamonti, and M. Vanali. ‘Beamforming method: Suppression of spatial aliasing using moving arrays.’ *2nd Berlin Beamforming Conference, 2008*, 2008.
- [7] C. S. Allen, W. K. Blake, R. P. Dougherty, D. Lynch, P. T. Soderman, and J. R. Underbrink. *Aeroacoustic measurements*. Springer-Verlag, 1 edition, 2002. ISBN 978-3-662-05058-3.
- [8] D. Ragni, F. Avallone, and D. Casalino. ‘Measurement techniques for aeroacoustics.’ *Measurement Science and Technology*, 33, 2022. doi:10.1088/1361-6501/ac547d.
- [9] C. Vandercreek, R. Merino-Martinez, P. Sijtsma, and M. Snellen. ‘Evaluation of the effect of microphone cavity geometries on acoustic imaging in wind tunnels.’ *Applied Acoustics*, 181, 108154, 2021. doi:10.1016/j.apacoust.2021.108154.
- [10] M. Remillieux, E. Crede, H. Camargo, R. Burdisso, W. Devenport, M. Rasnick, P. Seeters, and A. Chou. ‘Calibration and demonstration of the new virginia tech anechoic wind tunnel.’ 2008. doi:10.2514/6.2008-2911. 14th AIAA/CEAS Aeroacoustics Conference 5 - 7 May 2008, Vancouver, British Columbia Canada.
- [11] L. Santana, M. Carmo, and F. Catalano. ‘The update of an aerodynamic wind-tunnel for aeroacoustics testing.’ *Journal of Aerospace Technology and Management*, 6, 2014. doi:10.5028/jatm.v6i2.308.
- [12] H. Bento, C. VanderCreek, F. Avallone, D. Ragni, P. Sijtsma, and M. Snellen. ‘Wall treatments for aeroacoustic measurements in closed wind tunnel test sections.’ In *29th AIAA/CEAS Aeroacoustics Conference, June 12 – 16 2023, San Diego, CA, USA*. 2023. doi:10.2514/6.2023-4162. URL <http://arc.aiaa.org/doi/pdf/10.2514/6.2023-4162>, AIAA paper 2023–4162.
- [13] K. Brown, W. Devenport, and A. Borgoltz. ‘Exploitation of hybrid anechoic wind tunnels for aeroacoustic and aerodynamic measurements.’ *CEAS Aeronautical Journal*, 10, 251–266, 2019. doi:10.1007/s13272-019-00385-2. URL <https://doi.org/10.1007/s13272-019-00385-2>.
- [14] P. Sijtsma. ‘Feasibility of In-Duct Beamforming.’ In *13th AIAA/CEAS Aeroacoustics Conference (28th AIAA Aeroacoustics Conference)*. 2007.

- [15] P. Sijtsma, R. Merino-Martinez, A. M. N. Malgoezar, and M. Snellen. ‘High-Resolution CLEAN-SC: Theory and Experimental Validation.’ *International Journal of Aeroacoustics*, 16(4-5), 274-298, 2017. doi:10.1177/1475472X17713034. URL <http://journals.sagepub.com/doi/10.1177/1475472X17713034>, SAGE Publications Ltd. London, United Kingdom.
- [16] T. Brooks and W. Humphreys. ‘A deconvolution approach for the mapping of acoustic sources (damas) determined from phased microphone arrays.’ *Journal of Sound and Vibration*, 294(4), 856-879, 2006. ISSN 0022-460X. doi:<https://doi.org/10.1016/j.jsv.2005.12.046>. URL <https://www.sciencedirect.com/science/article/pii/S0022460X06000289>.
- [17] Y. Hinssen. *Enhancement of Aeroacoustic Testing: Applied to closed-section wind tunnels*. Master’s thesis, Delft University of Technology, 2024. URL <https://repository.tudelft.nl/islandora/object/uuid%3A53f55ed8-2cf3-4625-9071-28a3185029ee?collection=education>.
- [18] P. D. Welch. ‘The Use of Fast Fourier Transform for the Estimation of Power Spectra: A Method Based on Time Averaging Over Short, Modified Periodograms.’ *IEEE Transactions on Audio and Electroacoustics*, AU-15(2), 70-73, 1967. doi:10.1109/TAU.1967.1161901. URL <http://ieeexplore.ieee.org/stamp/stamp.jsp?arnumber=1161901>.
- [19] R. Merino-Martinez. *Microphone arrays for imaging of aerospace noise sources*. Ph.D. thesis, Delft University of Technology, Faculty of Aerospace Engineering, 2018. doi:10.4233/uuid:a3231ea9-1380-44f4-9a93-dbbd9a26f1d6.
- [20] R. Merino-Martinez, P. Sijtsma, A. Rubio Carpio, R. Zamponi, S. Luesutthiviboon, A. M. N. Malgoezar, M. Snellen, C. Schram, and D. G. Simons. ‘Integration methods for distributed sound sources.’ *International Journal of Aeroacoustics*, 18(4-5), 444-469, 2019. doi:10.1177/1475472X19852945. URL <https://doi.org/10.1177/1475472X19852945>.
- [21] R. Merino-Martínez, P. Sijtsma, M. Snellen, T. Ahlefeldt, J. Antoni, C. J. Bahr, D. Blacodon, D. Ernst, A. Finez, S. Funke, T. F. Geyer, S. Haxter, G. Herold, X. Huang, W. M. Humphreys, Q. Leclère, A. Malgoezar, U. Michel, T. Padois, A. Pereira, C. Picard, E. Saradj, H. A. Siller, D. G. Simons, and C. Spehr. ‘A review of acoustic imaging methods using phased microphone arrays.’ *CEAS Aeronautical Journal*, 10, 197-230, 2019.
- [22] J. Hald. ‘Cross-spectral matrix diagonal reconstruction.’ 2016. INTERNOISE 2016.